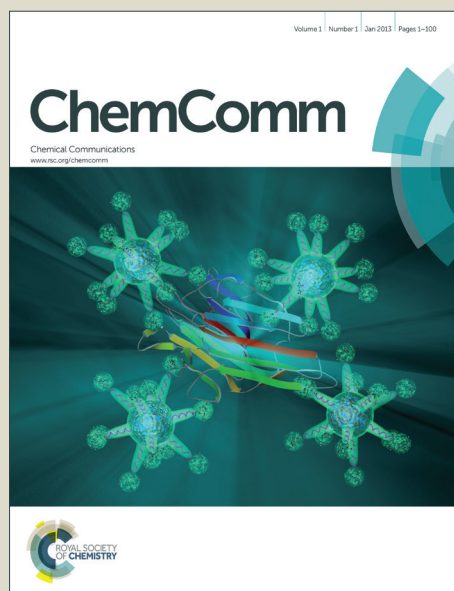


# ChemComm

Accepted Manuscript



This is an *Accepted Manuscript*, which has been through the Royal Society of Chemistry peer review process and has been accepted for publication.

*Accepted Manuscripts* are published online shortly after acceptance, before technical editing, formatting and proof reading. Using this free service, authors can make their results available to the community, in citable form, before we publish the edited article. We will replace this *Accepted Manuscript* with the edited and formatted *Advance Article* as soon as it is available.

You can find more information about *Accepted Manuscripts* in the [Information for Authors](#).

Please note that technical editing may introduce minor changes to the text and/or graphics, which may alter content. The journal's standard [Terms & Conditions](#) and the [Ethical guidelines](#) still apply. In no event shall the Royal Society of Chemistry be held responsible for any errors or omissions in this *Accepted Manuscript* or any consequences arising from the use of any information it contains.

# Polygermane: Bandgap Engineering via Tensile Strain and Side-Chain Substitution

Wei Fa<sup>a\*</sup> and Xiao Cheng Zeng<sup>b\*</sup>

Received (in XXX, XXX) XthXXXXXXXXXX 200X, Accepted Xth XXXXXXXXXXXX 200X

First published on the web Xth XXXXXXXXXXXX 200X

DOI: 10.1039/b000000x

Successful synthesis of the phenylisopropyl hexagermane (*Chem. Commun.* 2013, 49, 8380) offers exciting opportunity to synthesize a new class of low-dimensional germanium compounds with novel optical and electronic properties. Using the phenylisopropyl hexagermane as a model template, we have performed an *ab initio* study of electronic properties of polygermanes. Our density-functional theory calculations show that the polygermane is a quasi-one-dimensional semiconductor with a direct bandgap, and its valence and conduction bands are mainly contributed by the skeleton Ge atom. We have also explored effects of tensile and compressive strains and various side-chain substituents on the bandgap. The bandgap of polygermanes can be reduced upon attaching larger-sized substituents to the side chains. More importantly, applying a tensile/compressive strain can modify the bandgap of polygermanes over a wide range. For poly(diphenylgermane), the tensile strain can result in significant bandgap reduction due to increasingly delocalized charge density in the conduction band. Moreover, a strong compressive strain can induce a direct-to-indirect semiconductor transition owing to the change made in the band-edge states. Similar strain effect is seen in polystannanes as well.

Polymers and catenated compounds of the heavier group 14 elements have attracted growing interest due to their intriguing optical and electronic properties stemming from their inherent  $\sigma$ -delocalization. Their potential applications include photoconductors, optical materials, and non-linear optics.<sup>1-12</sup> Although synthesis and properties of silicon- and tin-containing polymers and oligomers have been intensively studied, those of the related germanium congeners have received less attention due in part to the challenge in obtaining germanium oligomers with suitably high yields. Nevertheless, the promise of new optical and electronic properties of organogermanium compounds, which may be enhanced relative to silicon-based analogues owing to the smaller band gap and higher electron and hole mobility in germanium, has prompted persistent efforts in their preparation and characterization.<sup>13-18</sup> Recently, a linear phenylisopropyl hexagermane,  $\text{Pr}_3\text{Ge}(\text{GePh}_2)_4\text{GePr}_3$ , has been successfully synthesized.<sup>19</sup> This  $\text{Ge}_6$  compound is the longest linear molecular oligogermane characterized to date, which can be viewed as a validation of the conjecture that discrete linear oligogermanes with sufficiently long Ge-Ge chains might exhibit similar properties to their polymeric analogues. For instance, like polygermanes,<sup>6</sup> the phenylisopropyl hexagermane exhibits fluorescence in the near UV region. Considering the linear  $\text{Ge}_6$  compound can serve as an effective oligomer model for long polygermane systems, it is interesting and timely to investigate the structural and electronic properties of polygermanes, especially poly(diphenylgermane)  $(\text{GePh}_2)_n$ . To this end, we have explored bandgap engineering in polygermanes by changing the substituents in the side chains or applying mechanical strains,

using first-principles density functional theory (DFT) calculations. Strain engineering is known as an effective approach to achieve continuously tunable bandgap as those successfully done in quasi-one-dimensional boron nitride (BN) nanoribbons and quasi-two-dimensional transition-metal dichalcogenides.<sup>20-25</sup> Moreover, the importance of strain engineering in germanium has also been demonstrated since tensile strain not only can increase the light emission efficiency but also tune the emission wavelength.<sup>26,27</sup> Here, we show that polygermanes is a quasi-one-dimensional semiconductor. Importantly, the bandgap of polygermanes can be tuned over a wide range by applying either tensile or compressive strains. Like other low-dimensional semiconducting materials, such as graphene or BN nanoribbons, relatively large strains may be applied onto the more flexible polygermanes to achieve wider tunability of bandgap. If confirmed experimentally, the strain engineering of the semiconducting polygermanes may be exploited for applications in nanoelectronic or optoelectronic devices.

Structure optimization was carried out using a three-dimensional periodic tetragonal supercell which contains four Ge atoms along the  $z$  axis to fully simulate the structural segments in the linear  $\text{Pr}_3\text{Ge}(\text{GePh}_2)_4\text{GePr}_3$ . DFT calculations are performed within the Perdew–Burke–Ernzerhof (PBE) generalized gradient approximation (GGA).<sup>28</sup> More computational details are given in the Electronic Supplementary Information (ESI). In addition, calculation results based on the more accurate hybrid HSE06 functional are also given in ESI, which confirm the trend of bandgap change predicted by the PBE calculations.

First, the atomic positions and  $z$ -lattice vector are relaxed to obtain the optimized geometry of  $(\text{GePh}_2)_n$ . Although Ge-Ge single-bond distance in discrete oligogermanes is typically within the range 2.43–2.49 Å (e.g., the recently reported value of 2.4710(3) Å for the hexagermane<sup>19</sup>), it is acceptable that the calculated average Ge-Ge bond distance in a unit cell of  $(\text{GePh}_2)_n$  is 2.549 Å, in view of overestimation of the bond lengths by PBE calculations.<sup>30</sup> The calculated average Ge-Ge-Ge bond angle of  $(\text{GePh}_2)_n$  is 115.16°, very close to the average value of 115.74(1)° measured in the  $\text{Pr}_3\text{Ge}(\text{GePh}_2)_4\text{GePr}_3$ .<sup>19</sup>

Next, the band structure of  $(\text{GePh}_2)_n$  was computed. As shown in Fig. 1(a), it is clear that the poly(diphenylgermane) is a semiconductor with a direct bandgap of 2.13 eV at the  $\Gamma$  point. By substituting the phenyl group(s) in  $(\text{GePh}_2)_n$  with H atom(s), poly(hydrophenylgermane)  $(\text{GeHPh})_n$  or poly(dihydrogermane)  $(\text{GeH}_2)_n$  is obtained. Their band structures are shown in Fig. 1 (b) and (c), respectively. Both exhibit a direct band gap, whose value is 2.72 and 3.03 eV, respectively. Thus, the bandgap can be reduced by several tenth of eV when larger substituents are attached. The band-edge states are mainly contributed by the skeleton Ge atomic orbital (AO). As shown by computed charge-density distributions and partial density of states (PDOSs) of Ge

atoms (Fig. 1), the lowest unoccupied molecular orbital (LUMO) is mainly contributed by the skeleton Ge  $4s$  and  $4p_x$  AOs while the highest occupied molecular orbital (HOMO) is composed mainly of the Ge  $4p_z$  (along the skeleton axis). So the bandgap reduction is relatively small even when the side-chain groups are changed dramatically from H to phenyl, which is similar to that for polysilanes whose band-edge states are mainly contributed by the skeleton Si AOs.<sup>31</sup> For  $(\text{SiXY})_n$ , the bandgap is 4.53, 3.73, and 3.61 eV for  $\text{XY} = \text{H}_2$ , HPh, and  $\text{Ph}_2$ , respectively.

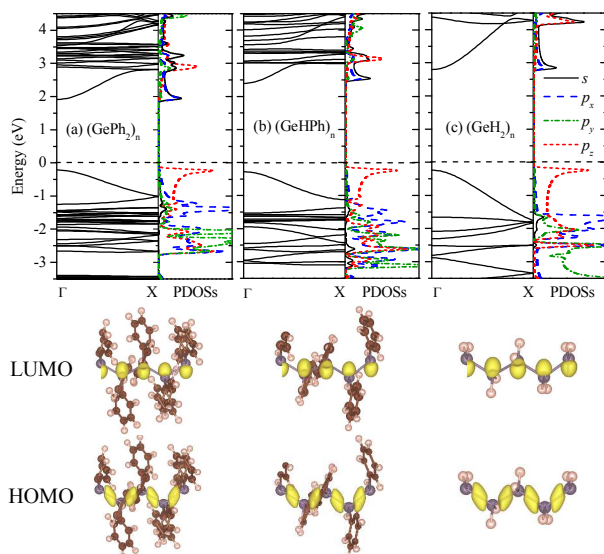
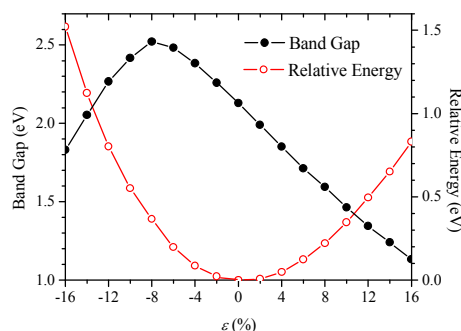


**Figure 1.** Computed band structures and PDOSs of Ge atoms in the unit cell of (a)  $(\text{GePh}_2)_n$ , (b)  $(\text{GeHPh})_n$ , and (c)  $(\text{GeH}_2)_n$ . The  $s$ ,  $p_x$ ,  $p_y$ , and  $p_z$  PDOSs are denoted by solid, dashed, dash dot, and short dashed lines, respectively. The purple, brown, and pink balls represent Ge, C, and H atoms, respectively. The Fermi level is marked by a horizontal dashed line. The lower panels illustrate the charge-density distributions of HOMO and LUMO bands, respectively. The isosurface value is  $0.008 \text{ e/\AA}^3$ .

As noted above, the average Ge-Ge bond lengths of  $(\text{GeHPh})_n$  and  $(\text{GeH}_2)_n$  are 2.469 and 2.451 Å, respectively, both shorter than that of  $(\text{GePh}_2)_n$ . When larger functional groups are substituted in the side chains, the average Ge-Ge bond lengths are expected to be longer, which is likely responsible for the slight reduction of bandgap. Thus, we speculate that applying mechanical strains to the skeleton Ge chains may be an effective way to tune the bandgap of polygermanes. Compared to bulk materials, low-dimensional materials often allow a larger dynamic range for elastic strain.<sup>22</sup> For example, a maximum elastic strain even over 20% was predicted for the boron nitride nanoribbon systems.<sup>32</sup>

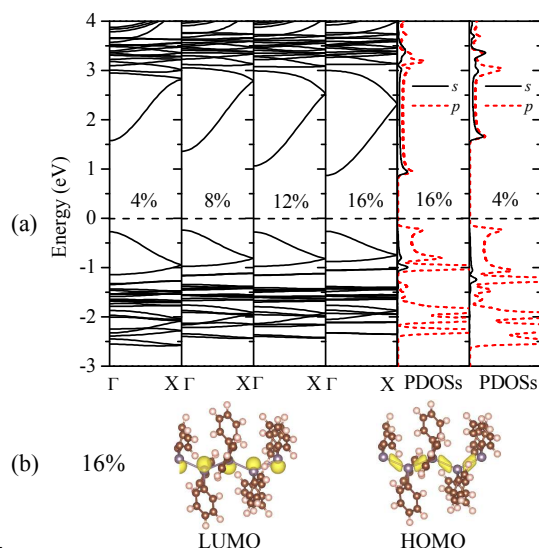
Figure 2 displays computed relative energies and bandgaps of  $(\text{GePh}_2)_n$  with respect to uniaxial strain along the  $z$ -direction. The strain  $\varepsilon$  is defined as  $\varepsilon = (c - c_0)/c_0\%$ , where  $c$  and  $c_0$  are the  $z$ -lattice parameters with and without the deformation. Clearly, the change in relative energies exhibits a monotonically increased tendency for both compressive and tensile strains, indicating that the wide strain range considered is elastic, namely, no structural transition or breakage occurs in the strain range considered. In this strain range, a monotonic decrease of bandgaps with strains is observed. For example, the 16% tensile strain reduces the bandgap of  $(\text{GePh}_2)_n$  to 1.131 eV, about a half of the bandgap of unstrained  $(\text{GePh}_2)_n$ . Hence, the bandgap of poly(diphenylgermane) can be broadly tuned by applying uniaxial elastic strains. Under

compressing, the bandgap is enlarged initially until  $\varepsilon = -8\%$ , then decreased with further increase of the compressive strain. To understand origin of this strain dependence of bandgap, computed band structures and charge density at different strains are shown in Figs. 3 and 4.



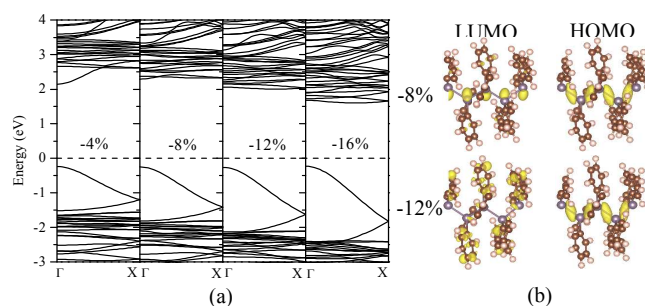
**Figure 2.** Computed bandgap and relative energy of  $(\text{GePh}_2)_n$  vs strain  $\varepsilon$ . Strain is applied to the optimized structure ( $\varepsilon = 0$ ) through uniaxial deformation in  $z$ -direction, for which negative  $\varepsilon$  represents compression and positive tensile strain.

Figure 3(a) shows that the direct-bandgap character of  $(\text{GePh}_2)_n$  is still retained under different uniaxial tensile strains. As the tensile strain increases, the HOMO band exhibits little changes, while the LUMO band is relocated closer to the Fermi level, leading to reduced bandgaps. The computed PDOSs offer more insights into the mechanism of bandgap reduction induced by the tensile strains. Comparing the PDOSs shown in Fig. 3(a), the conduction band bottom states span over a broader energy range ( $\sim 1.5 \text{ eV}$ ) at  $\varepsilon = 16\%$  than that ( $\sim 1.2 \text{ eV}$ ) at  $\varepsilon = 4\%$ , consistent with their band structures. Thus, at higher tensile strains, the LUMO states are more delocalized due to the extended Ge-Ge bond lengths. For HOMO, however, no alteration is seen in the corresponding charge densities at different tensile strains. As shown in Fig. 3(b), even the tensile strain reaches 16%, charge density distributions in the band-edge states remain the same skeleton-Ge characteristics. We thus conclude that the increase of the average Ge-Ge bond length in polygermanes leads to increasingly delocalized conduction band bottom states and thus reduced bandgaps.



**Figure 3.** Computed (a) band structure of  $(\text{GePh}_2)_n$  under different uniaxial tensile strains. PDOSs of Ge atoms at the strains of 4 and

16% are displayed for comparison; (b) charge densities of HOMO and LUMO states at  $\varepsilon = 16\%$ .



**Figure 4.** Computed (a) band structure of  $(\text{GePh}_2)_n$  under different uniaxial compressive strains; (b) charge densities corresponding to HOMO and LUMO states at  $\varepsilon = -8$  or  $\varepsilon = -12\%$ .

A similar mechanism is applicable for relatively weak compressive strains (up to  $\varepsilon = -8\%$ ), at which the compressed  $(\text{GePh}_2)_n$  still exhibits a direct bandgap with the band-edge states of Ge AOs given in Fig. 4. The enlarged bandgap from 2.129 to 2.522 eV under the compressive strain from 0 to  $-8\%$  can be related to the decreased average Ge-Ge bond length from 2.549 to 2.479 Å and thereby the upward shift of the lowest conduction band. For the compressive strain beyond  $-8\%$ , the bandgap is reduced and changed to an indirect gap. By analysis of charge densities of HOMO and LUMO states, it can be seen from Fig. 4(b) that although the HOMO state still stems from the skeleton Ge  $4p_z$  orbitals, the LUMO state is mainly contributed from the side-chain substituents for the compressive strain beyond  $-8\%$ . Thus, the bandgap reduction under higher compressive strains is due to the variation of band-edge states. In passing, we note that polystannanes possess qualitatively similar electronic properties with either side-chain substituents or under mechanical strains. Results of strain engineering of bandgap are given in ESI.

In conclusion, we have performed DFT calculations to study effects of side-chain substitution and mechanical strains on the electronic properties of polygermanes. Polygermanes exhibit the direct bandgap character and their band-edge states are attributed mainly to skeleton Ge, which can lead to relatively small bandgap reduction when the side-chain groups are changed from H to phenyl. On the other hand, the bandgap of polygermanes can be tuned over much broader range by applying mechanical strains. It is found that under the tensile strains, the bandgap of  $(\text{GePh}_2)_n$  decreases with the increase of strain since the conduction band bottom states become more delocalized. Compressive strains up to  $-8\%$  can enlarge the bandgap. Further increase of the compressive strain results in the direct-to-indirect bandgap transition with gradually reduced bandgap due to the variation of band-edge states.

We are grateful for valuable discussions with Drs. Shuang Chen, and Ning Lu. WF acknowledged the Natural Science Foundation of China under No. 11074107, the State Scholarship Fund provided by the China Scholarship Council through No. 201308320156, and computing support by High Performance Computing Center of Nanjing University. XCZ is supported by ARL (Grant No. W911NF1020099) and UNL Holland Computing Center.

## Notes and references

<sup>a</sup>National Laboratory of Solid State Microstructures and Department of Physics, Nanjing University, Nanjing, 210093, China. E-mail: wfa@nju.edu.cn

<sup>b</sup>Department of Chemistry, University of Nebraska-Lincoln, Lincoln, Nebraska, 68588, USA. E-mail: xzeng1@unl.edu

†Electronic supplementary information (ESI) available: Computational details; comparison using the LDA and GGA exchange-correlation functionals; results of the hybrid HSE06 functional calculations; GGA results of electronic properties of polystannanes and effects of mechanical strains.

- R. D. Miller and J. Michl, *Chem. Rev.*, 1989, **89**, 1359-1410.
- R. G. Jones and S. J. Holder, *Polym. Int.*, 2006, **55**, 711-718.
- T. Hayashi, Y. Uchimar, N. P. Reddy and M. Tanaka, *Chem. Lett.*, 1992, 647-650.
- J. -C. Baumert, G. C. Bjorklund, D. H. Jundt, M. C. Jurich, H. Looser, R. D. Miller, J. Rabolt, R. Sooriyakumaran, J. D. Swalen and R. J. Twieg, *Appl. Phys. Lett.*, 1988, **53**, 1147-1149.
- T. Kodaira, A. Watanabe, O. Ito, M. Matsuda, S. Tokura, M. Kira, S. Nagano and K. Mochida, *Adv. Mater.*, 1995, **7**, 917-919.
- Y. Huo and D. H. Berry, *Chem. Mater.*, 2005, **17**, 157-163.
- J. -P. Majoral and A. -M. Caminade, *Chem. Rev.*, 1999, **99**, 845-880.
- M. L. Amadoruge and C. S. Weinert, *Chem. Rev.*, 2008, **108**, 4253-4294.
- Y. Y. Durmaz, M. Kukut, N. Monszner and Y. Yagci, *Macromolecules*, 2009, **42**, 2899-2902.
- M. Okano, N. Matsumoto, M. Arakawa, T. Tsuruta and H. Hamano, *Chem. Commun.*, 1998, 1799-1800.
- F. Choffat, P. Smith and W. Caseri, *Adv. Mater.*, 2008, **20**, 2225-2229.
- M. Trummer, F. Choffat, P. Smith and W. Caseri, *Macromol. Rapid Commun.*, 2012, **33**, 448-460.
- T. Azemi, Y. Yokoyama and K. Mochida, *J. Organomet. Chem.*, 2005, **690**, 1588-1593.
- M. L. Amadoruge, J. A. Golen, A. L. Rheingold and C. S. Weinert, *Organometallics*, 2008, **27**, 1979-1984.
- M. L. Amadoruge, A. G. DiPasquale, A. L. Rheingold and C. S. Weinert, *J. Organomet. Chem.*, 2008, **693**, 1771-1778.
- C. S. Weinert, *Dalton Trans.*, 2009, 1691-1699.
- E. K. Schrick, T. J. Forget, K. D. Roewe, A. C. Schrick, C. E. Moore, J. A. Golen, A. L. Rheingold, N. F. Materer and C. S. Weinert, *Organometallics*, 2013, **32**, 2245-2256.
- Y. Matsuura, *J. Appl. Phys.*, 2014, **115**, 043701.
- K. D. Roewe, A. L. Rheingold and C. S. Weinert, *Chem. Commun.*, 2013, **49**, 8380-8382.
- F. Guinea, M. I. Katsnelson, and A. Geim, *Nat. Phys.*, 2010, **6**, 30-33 (2010).
- Z. H. Ni, T. Yu, Y. H. Lu, Y. Y. Wang, and Y. P. Feng, *ACS Nano*, 2008, **11**, 2301-2305.
- T. Zhu and J. Li, *Prog. Mater. Sci.*, 2010, **55**, 710-757.
- J. Qi, X. Qian, L. Qi, J. Feng, D. Shi and J. Li, *Nano Lett.*, 2012, **12**, 1224-1228.
- P. Johari and V. B. Shenoy, *ACS Nano*, 2012, **6**, 5449-5456.
- N. Lu, H. Guo, L. Li, J. Dai, L. Wang, W. -N. Mei, X. Wu and X. C. Zeng, *Nanoscale*, 2014, **6**, 2879-2886.
- J. R. Sánchez-Pérez, C. Boztug, F. Chen, F. F. Sudradjat, D. M. Paskiewicz, R. B. Jacobson, M. G. Lagally and R. Paiella, *Proc. Natl. Acad. Sci.*, 2011, **108**, 18893-18898.
- M. J. Süess, R. Geiger, R. A. Minamisawa, G. Schiefler, J. Frigerio, D. Chrastina, G. Isella, R. Spolenak, J. Faist and H. Sigg, *Nature Photonics*, 2013, **7**, 466-472.
- J. P. Perdew, K. Burke and M. Ernzerhof, *Phys. Rev. Lett.*, 1996, **77**, 3865-3868.
- M. Dräger, L. Ross and D. Simon, *Rev. Silicon, Germanium, Tin, Lead compds.*, 1983, **7**, 299.
- K. Y. Kim, D. Cho, B. Cheong, D. Kim, H. Horii and S. Han, *J. Appl. Phys.*, 2013, **113**, 134302.
- K. Takeda, H. Teramae and N. Matsumoto, *J. Am. Chem. Soc.*, 1986, **108**, 8186-8190.
- M. Topsakal and S. Ciraci, *Phys. Rev. B*, 2010, **81**, 024107.